

1 This manuscript is a preprint and has not been peer-reviewed. Please feel free to contact any of the
2 authors; we welcome feedback

3 **Microbial lipid signatures in Arctic deltaic sediments - insights into**
4 **methane cycling and climate variability**

5 **Julie Lattaud^{1*}, Cindy De Jonge¹, Ann Pearson², Felix J. Elling², Timothy I. Eglinton¹**

6

7 ¹Biogeosciences Group, ETH Zurich, Sonneggstrasse 5, Zurich, Switzerland

8 ²Department of Earth and Planetary Sciences, Harvard University, Cambridge, MA 02138,
9 USA

10

11 ***Correspondance:**

12 Julie Lattaud

13 jlattaud@ethz.ch

14

15 **Abstract.**

16 Glycerol Dialkyl Glycerol Tetraethers (GDGTs) are ubiquitous biomolecules whose structural
17 diversity or isotopic composition is increasingly used to reconstruct environmental changes
18 such as air temperatures or $p\text{CO}_2$. Isoprenoid GDGTs, in particular GDGT-0, are
19 biosynthesized by a large range of Archaea. To assess the potential of GDGT-0 as a tracer of
20 past methane cycle variations, three sediment cores from the Mackenzie River Delta have been
21 studied for iGDGT and diploptene distribution and stable carbon signature. The absence of
22 crenarchaeol, high GDGT-0 vs crenarchaeol ratio, and ^{13}C -enriched carbon signature of
23 GDGT-0 indicate production by acetoclastic methanogens as well as heterotrophic Archaea.
24 The oxidation of methane seems to be dominated by bacteria as indicated by the high
25 abundance of ^{13}C -depleted diploptene. Branched GDGTs, thought to be produced by
26 heterotrophic bacteria, are dominated by hexa- and penta-methylated 5- and 6-methyl
27 compounds. The presence of 5,6-methyl isomer IIIa'' points towards in situ production of
28 brGDGTs, with only a minor input from soil branched GDGT brought by the Mackenzie River.
29 Carbon isotopic compositions of brGDGTs are in agreement with heterotrophic producers,
30 likely living during summer. The reconstructed temperatures using a global lake calibration
31 reflect recorded summer air temperature ($\pm 2.14\text{ }^\circ\text{C}$) during the last 60 years, and further
32 highlight the absence of warming in summer in this region during the last 200 years. Oxygen
33 availability and connection time to the Mackenzie River also seem to control the distribution
34 of branched GDGT with an increase in 6-methyl and 5,6-methyl isomers with increased period
35 of anoxia.

36 **Keywords: GDGT, methane cycle, Mackenzie River, temperature reconstruction, carbon**
37 **isotopes**

38

39 **1 Introduction**

40 The Mackenzie delta region in the Canadian Arctic is highly sensitive to climate change, and
41 has already recorded a warming of 6 °C in mean annual temperature since 1970 (based on
42 Environment and Climate Change Canada). This warming exclusively manifests itself in winter
43 temperature, whereas the summer temperature has been stable (based on Environment and
44 Climate Change Canada). The Mackenzie River delta is characterized by thousands of small
45 shallow lakes (mean depths from about 0.5 m to 4.5 m) (Emmerton et al., 2007) that are frozen
46 from late September to early June (Droppo et al., 1998). These lakes are connected with the
47 main river channels to different degrees and have been classified into three categories by
48 Lesack and Marsh (2007): “No closure” lakes are continuously linked to the river, “low
49 closure” lakes have a connection that occurs at least once a year during the freshet, and “high
50 closure lakes”, characterized by a higher levees, are only connected to the river during extreme
51 freshets, with recurrence intervals that may be only once per decade. Most inland water bodies
52 of the Mackenzie River delta are a net sink of carbon dioxide (CO₂) and a source of methane
53 (CH₄) (Tank et al., 2008). However, inland water bodies are highly sensitive to temperature
54 changes, as warming will strongly impact water column stratification, aquatic ecosystems as
55 well as the gas exchange dynamics of the lakes. To understand the impact of these arctic
56 wetlands on global greenhouse gas budgets, and project the long-term evolution of this
57 environment, constraining the effects of warming on aquatic ecosystems of the region is
58 essential.

59 Archaeal and bacterial membrane-spanning lipids, glycerol dialkyl glycerol tetraethers
60 (GDGTs) are ubiquitous biomarkers that are found in extreme environments such as
61 perennially frozen soils, e.g., Siberian permafrost (Kusch et al., 2019), and in surface lake
62 sediments of the Mackenzie delta (Peterse et al., 2014). Isoprenoid GDGTs (iGDGTs) are
63 biosynthesized by a wide range of Archaea, with some iGDGTs such as crenarchaeol and

64 crenarchaeol regioisomer having a narrow phylogenetic source, i.e., ammonia-oxidizing
65 Thaumarchaeota (Schouten et al., 2013). In contrast, GDGT-0 is found in many cultivated
66 strains of Archaea (Oger and Cario, 2013; Schouten et al., 2013; Villanueva et al., 2014; Elling
67 et al., 2017), but it is particularly abundant in methanogens and methanotrophs (Koga et al.,
68 1993; Pancost et al., 2001; Bauersachs et al., 2015; Sollai et al., 2019). In marine and freshwater
69 realms, GDGT-0 has been used as an indicator of the presence of methanotrophic and
70 methanogenic Archaea. Several ratios have been built to infer the emission of CH₄ such as the
71 methane index (Zhang et al., 2011), or the relative abundance of GDGT-0 versus crenarchaeol
72 (Blaga et al., 2009). Carbon isotopic measurements of iGDGTs have also shed light on the
73 influence of Archaea on methane cycling in lacustrine and marine environments as the stable
74 carbon isotopic composition of lipids reflect the carbon source of the producer, and methane is
75 usually ¹³C-depleted (Pancost et al., 2000; Sinninghe Damsté et al., 2009a; Weber et al., 2015;
76 Colcord et al., 2017). Methyl-branched GDGTs (brGDGTs) are ubiquitous bacterial membrane
77 lipids that are abundant in soils (e.g., De Jonge et al., 2014a; Weijers et al., 2007) and lakes
78 (e.g., Blaga et al., 2009; Colcord et al., 2015; Dang et al., 2016; Foster et al., 2016; Russell et
79 al., 2018). In soils, they are inferred to be produced by members of the phylum Acidobacteria,
80 based on cultures (Sinninghe Damsté et al., 2014, 2018) and on their environmental distribution
81 (Weijers et al., 2010). In lakes, they are likely produced by multiple groups of bacteria (Weber
82 et al., 2018). The degree of methylation of the brGDGTs reflects an adaptation to temperature,
83 with higher fractional abundance of hexa- and pentamethylated GDGTs (GDGT-II and GDGT-
84 III) in colder soils (Weijers et al., 2007; Jonge et al., 2014; Colcord et al., 2015; Zink et al.,
85 2016), and permafrost soils dominated by GDGT-IIIa (Kusch et al., 2019). BrGDGTs can be
86 recovered from geological archives such as paleosoils or lacustrine sediments, but their dual
87 provenance in lake sediments can be problematic as the relative abundances of brGDGTs in
88 soils has been shown to differ from those in lake sediments under the same temperature (e.g.,

89 Martin et al., 2020; Tierney and Russell, 2009; Zink et al., 2016). The source of brGDGTs can
90 thus be inferred by investigating the distribution of the brGDGTs. In marine coastal
91 environments, three ratios have been developed: the weighted average number of cyclopentane
92 moieties and the degree of methylation of the brGDGTs (Sinninghe Damsté, 2016), the ratio
93 of GDGT-IIIa over GDGT-IIa (Xiao et al., 2016), and the BIT index (Hopmans et al., 2004).
94 In freshwater environments, only the ratio of GDGT-IIIa/GDGT-IIa has thus far been used to
95 assess the origin of brGDGTs, utilizing values for modern soils and lake sediments (Martin et
96 al., 2019). In addition, compound-specific ^{13}C values (Weijers et al., 2007; Naeher et al., 2014a;
97 Colcord et al., 2017; Weber et al., 2018) have been proposed to as a means to distinguish lake-
98 or soil-derived sources through comparison with ^{13}C values of bulk organic carbon (OC) and
99 other biomarkers. Once the provenance is determined, corresponding lacustrine or soil
100 calibration can be applied, with numerous studies constructing a local, region-specific
101 calibration using lake surface sediments or suspended particulate matter (SPM, e.g., Foster et
102 al., 2016; Pearson et al., 2011; Sun et al., 2011; Tierney et al., 2010; Zink et al., 2016) or other
103 proxies such as pollen (Dugerdil et al., 2020) or haptophyte biomarkers (Harning et al., 2020).
104 Alternatively, calibration based on large spatial scale variations (Loomis et al., 2012; Russell
105 et al., 2018) can be used. Soil-specific calibrations have also been constructed (De Jonge et al.,
106 2014b; Peterse et al., 2012; Watson et al., 2018), and have been found to yield reliable results
107 in temperate environments.

108 Peterse et al. (2014) determined that most of the brGDGTs in Mackenzie delta lake surface
109 sediments originated from in situ production within the lakes. This contrasted sharply with the
110 Mackenzie River where most of the brGDGTs originated from erosion and transport of soils
111 within the catchment. Here, we investigate three sediment cores retrieved from lakes in the
112 middle (MD-1 and MD-2) and upper delta (UD-4) that have previously been studied from a
113 sedimentological and biogeochemical perspective (*n*-alkanes and fatty acid biomarkers, bulk

114 OC ¹⁴C and ¹³C) (Lattaud et al. submitted). The core-tops of these lakes have previously been
115 examined by Vonk et al. (2015) as part of a study to assess sediment dispersal and deposition
116 patterns in the Mackenzie delta. Based on these prior investigations it was determined that low
117 closure lakes have the clear potential to record past climate changes. Here, we use brGDGTs
118 determine the provenance and assess climate signals recorded (last 200 yr) in one low closure
119 lake (UD-4) in comparison with a no closure (MD-2) and a high closure (MD-1) lake.
120 Furthermore, iGDGTs and their stable carbon isotopes are studied to investigate past methane
121 cycling in these lakes.

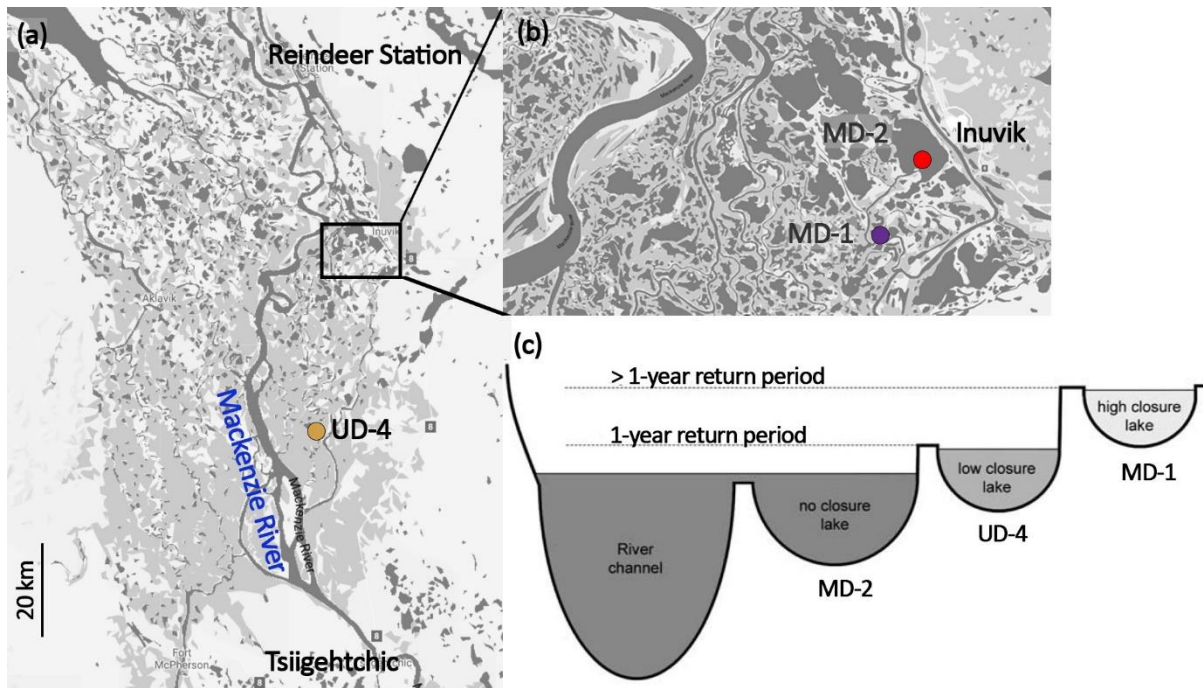
122

123 **2 Material and methods**

124 **2.1 Study sites**

125 The Mackenzie delta is located in the Canadian arctic, at latitudes above 67°N (Fig. 1), with a
126 subpolar drainage basin that lies primarily (~75%) within the continuous and discontinuous
127 permafrost zones. Within the central Mackenzie Delta (i.e., the area between Aklavik and
128 Inuvik), summers are cool and short, with ice-free conditions lasting from early June to late
129 September. The mean summer (June – August) and winter (November – February) air
130 temperature for Inuvik are 11.4 °C and -25.5 °C, respectively (based on Environment and
131 Climate Change Canada) with a mean annual (MAT) average of -9.2 °C. The MAT in the south
132 of the basin is much warmer, averaging 0.7 °C at Fort McMurray. The Mackenzie River flows
133 northward from areas of relative warmth toward frozen northern regions. It crosses several
134 large lakes such as Great Slave Lake and Great Bear Lake that act as efficient sediment traps
135 (Carson et al., 1998; Carrie et al., 2009), and consequently most of the sediment reaching the
136 Mackenzie delta originates north of these lakes. The freshet, i.e. spring flood, which removes
137 snow cover from terrestrial surfaces, warming the ground and accelerating active-layer

138 development (Mackay, 1963), accounts for 60% and 90% of annual water and sediment
139 discharge, respectively (Drenzek et al., 2007), and is responsible for seasonal inundation of
140 lakes within the delta.



141 **Figure 1** (a) Localization of the Mackenzie delta lakes with (b) zoom of Inuvik area insert and
142 (c) diagram illustrating the degree of closure of the lakes.

143

144 Three representative lakes were chosen for the present study: MD-1, a high closure lake in the
145 middle delta with an area of ~ 5.9 ha and a mean depth of 0.74 m; UD-4, a low closure lake
146 from the upper part of the delta (surface area, ~ 12.5 ha; mean depth, 2.2 m), and MD-2, a no
147 closure lake close to Inuvik in the middle delta (surface area, ~ 700 ha; mean depth, 2.2 m)
148 (Lesack and Marsh, 2010; Vonk et al., 2015). These lakes have been previously studied for
149 their sedimentological properties (Lattaud et al., submitted) and have not always been in the
150 same connection state as now. Specifically, UD-4 was high closure before transitioning to low
151 closure before ca. 1890 C.E. (i.e., below 90 cm), while MD-2 was low closure before ca. 1928
152 C.E. (i.e., below 110 cm).

153 **2.2 Methods**

154 **2.2.1 Lakes sampling**

155 Mackenzie delta lake sediment cores were sampled in March 2009 with a push-corer (system
156 built in-house at the Geology and Geophysics department, Woods Hole Oceanographic
157 Institution, WHOI) as described by Vonk et al. (2015). Cores were shipped in cooled
158 conditions, split lengthwise and sliced every centimetre.

159 **2.2.2 Lipid extraction and analysis**

160 The sediments were freeze-dried and subsequently extracted with the EDGE system as
161 described in Lattaud et al. (submitted). Briefly, the total lipid extract was saponified, the neutral
162 fraction liquid-liquid extracted, and separated on a silica gel column into three fractions. The
163 polar fraction was filtered using a polytetrafluoroethylene 0.45 µm filter prior to analysis. As
164 GDGTs in the environment have predominantly glycosidic bounds, they are not cleaved to core
165 GDGTs by base hydrolysis (done in this study). Hence, the fraction of GDGTs analysed in this
166 study are mostly fossilized core GDGTs, plus a small fraction of the intact polar lipid GDGT
167 pool.

168 The GDGTs were analysed with high performance liquid chromatography (LC)/atmospheric
169 pressure chemical ionization–mass spectrometry (MS) on an Agilent 1260 Infinity series LC-
170 MS according to Hopmans et al. (2016). Selective ion monitoring of the $[M + H]^+$ was used to
171 detect and quantify the different GDGTs, according to Huguet et al. (2006), except that a
172 similar response factor was assumed for the GDGTs and the internal standard.

173 Diploptene was quantified on a HP 7890A gas chromatograph (GC) equipped with a flame
174 ionization detector (FID), and a VF-1 MS capillary column (30 m × 0.25 mm, 0.25 µm film
175 thickness). The temperature program started with a 1 min hold time at 50 °C, followed by a

176 10 °C min⁻¹ ramp to 320 °C and a 5 min hold time at 320 °C. Quantification was based on an
177 internal standard (C₃₆ *n*-alkane) of known concentration.

178 **2.2.3. GDGT carbon isotopic analysis**

179 Before stable carbon isotope analysis, GDGTs from MD-2 and UD-4 were isolated from the
180 polar fraction using semi-preparative normal phase HPLC following the method of Gies et al.
181 (2020). Fractions were collected from 16 to 18 min for GDGT-0 and 36 to 48 min for the
182 brGDGTs.

183 GDGTs from MD-1 were purified using semi-preparative normal phase HPLC following the
184 method of Pearson et al. (2016).

185 Purity of the prepped fractions was assessed using HPLC flow injection analysis (FIA) relative
186 to a dilution series of the C₄₆-GDGT standard (Huguet et al., 2006). ¹³C measurements of the
187 GDGT were performed at Harvard University as described in Pearson et al. (2016). In
188 summary, the GDGT fractions are purified by reverse phase (RP) HPLC to remove non-GDGT
189 material and the fractions containing the isolated GDGT (F2) and the minute before (F1) were
190 collected.

191 Values of δ¹³C_{GDGT} are measured by Spooling Wire Microcombustion-IRMS (SWiM-IRMS;
192 Pearson et al., 2016; Sessions et al., 2005). The precision measurements was ± 0.2‰. The ratio
193 of F2/F1 indicates the level of background contamination in a sample with low ratio (< 2)
194 indicating possible contamination.

195

196 **2.2.4. Diploptene carbon isotopic analysis**

197 The carbon isotope composition of diploptene was measured in duplicate by Gas
198 Chromatography-isotope ratio mass spectrometry (GC-IRMS) on a Thermo Trace GC (1310)
199 coupled with a Thermo Delta-V plus system at the Climate Geology group at ETH Zurich. The

200 GC was equipped with a RTX-200 MS capillary column (60 m × 0.25 mm i.d., 0.25 μm film
201 thickness) and temperature program was as follows: ramp from 40 °C to 120 °C at 40 °C min⁻¹,
202 followed by a 6 °C min⁻¹ ramp to 300 °C and 12 min hold time at 320 °C. Duplicates were
203 measured when possible.

204 **3. Results**

205

206 **3.1. GDGTs and diploptene distribution**

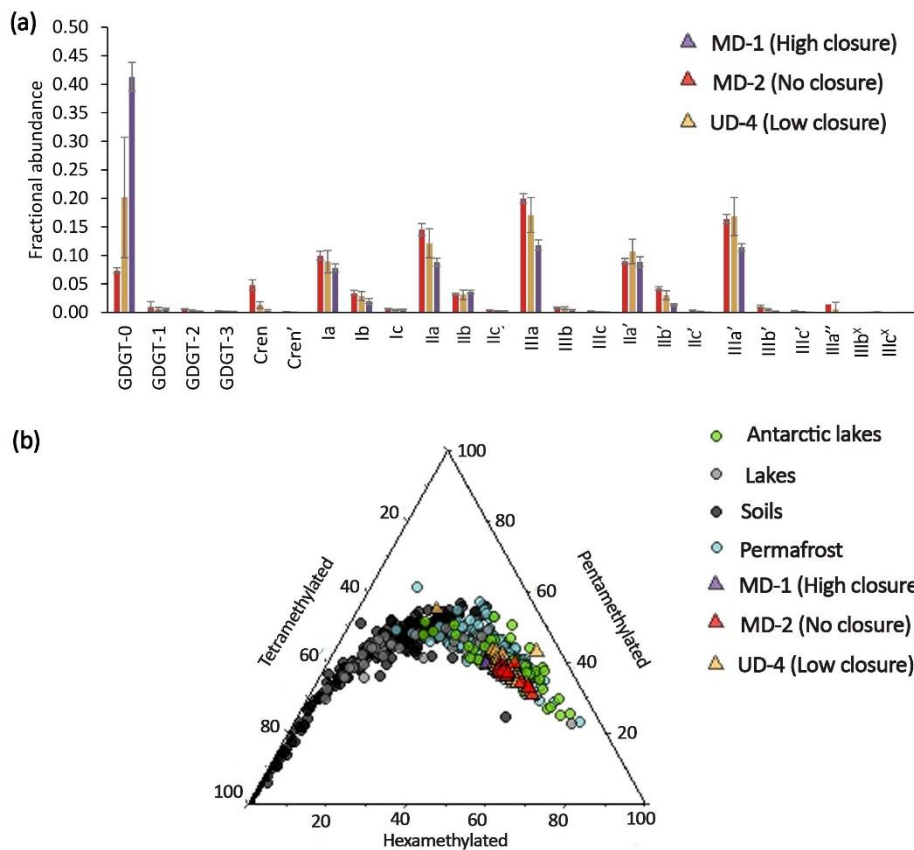
207 **3.1.1. iGDGT**

208 The isoprenoid GDGTs are dominated by GDGT-0 (Fig. 2), especially in MD-1 (high closure)
209 where it accounts for 90 ± 2% of all iGDGTs. GDGT-0 comprises 49 ± 4% of iGDGTs in MD-
210 2 (no closure) and 80 ± 12% of iGDGTs in UD-4 (low closure). The total amount of iGDGT is
211 higher in MD-1 (18.5 ± 17.7 μg g_{TOC}⁻¹) followed by UD-4 (10.8 ± 7.2 μg g_{TOC}⁻¹) and MD-2
212 (6.8 ± 3.6 μg g_{TOC}⁻¹), largely due to the increased abundance in GDGT-0. Only trace amounts
213 of crenarchaeol and crenarchaeol isomer are detected in all lakes (0.01 – 0.6 μg g_{TOC}⁻¹ in MD-
214 1, 0.01 – 0.1 μg g_{TOC}⁻¹ for UD-4 and 0.1 – 4 μg g_{TOC}⁻¹ for MD-2).

215 **3.1.2. BrGDGTs**

216 All sampled lakes have a similar distribution of brGDGT lipids (Fig. 2), with brGDGT-IIIa and
217 GDGT-IIIa' as the most abundant components, followed by GDGT-IIa, GDGT-Ia and GDGT-
218 IIa'. In MD-2 lake sediments (no closure), hexamethylated, pentamethylated and
219 tetramethylated components represent 46 ± 2%, 38 ± 2% and 17 ± 1%, respectively, of all the
220 brGDGT (15 brGDGT are quantified, see appendix 1). Similar distributions are encountered in
221 the other lake sediments, with 47 ± 5%, 38 ± 3% and 16 ± 2% for UD-4 (low closure), and 43
222 ± 2%, 40 ± 1% and 18 ± 1% for MD-1 (high closure) (hexa, penta and tetramethylated
223 compounds, respectively). Structural isomers of the hexamethylated compounds exhibit
224 different patterns among the lakes, with GDGT-IIIc X-methyl (structure not identified,

225 compound eluting between the GDGT-IIIc and GDGT-IIIc^X, further called the IIIc^X) present in
 226 MD-2, while IIIa'' and IIIc^X are found in UD-4, and GDGT-IIIb X-methyl (structure not
 227 identified, compound eluting between the GDGT-IIIb and GDGT-IIIb', IIIb^X) is present in
 228 MD-1. The concentration of brGDGTs is similar between MD-1 and MD-2 but is more variable
 229 ($22.5 \pm 21.5 \mu\text{g g}_{\text{TOC}}^{-1}$ and $19.2 \pm 10.4 \mu\text{g g}_{\text{TOC}}^{-1}$, respectively) and higher in UD-4 (33.7 ± 29.0
 230 $\mu\text{g g}_{\text{TOC}}^{-1}$).



231
 232 **Figure 2** GDGT composition in Mackenzie delta lakes (a) fractional abundance and (b) ternary
 233 diagram of the hexa-, penta- and tetra-methylated branched GDGT in Mackenzie lakes in
 234 comparison with a global lakes and soils dataset (Pearson et al., 2011 for lakes, Foster et al.
 235 2016 for Antarctic lakes and De Jonge et al., 2014b for soils).

236

237 3.1.3. Diploptene

238 Diploptene ($17\beta(\text{H}), 21\beta(\text{H})\text{-hop-22 (29)-ene}$) is detected at all depths in UD-4 (low closure)
239 and MD-1 (high closure), and at some depths in MD-2 (no closure). Its concentration is higher
240 in MD-1 and UD-4 than in MD-2 ($110 \pm 50 \mu\text{g g}_{\text{TOC}}^{-1}$, $130 \pm 80 \mu\text{g g}_{\text{TOC}}^{-1}$ and $50 \pm 20 \mu\text{g g}_{\text{TOC}}^{-1}$
241 1 respectively). The concentration of diploptene in MD-1 increases from the oldest part of the
242 record towards the top, reaching a maximum around 14 cm ($200 \mu\text{g g}_{\text{TOC}}^{-1}$). In UD-4 the
243 concentration is higher in the oldest part of the core, around 90 cm (reaching $340 \mu\text{g g}_{\text{TOC}}^{-1}$)
244 before decreasing until 28 cm (lowest concentration $40 \mu\text{g g}_{\text{TOC}}^{-1}$), and then increasing again
245 to the top of the core. Diploptene concentration in MD-2 is higher at the bottom of the core
246 ($140 \mu\text{g g}_{\text{TOC}}^{-1}$) then decreases and remains stable until the core top (average of $40 \pm 20 \mu\text{g}$
247 $\text{g}_{\text{TOC}}^{-1}$, $n = 64$).

248

249 **3.2. Carbon isotopes**

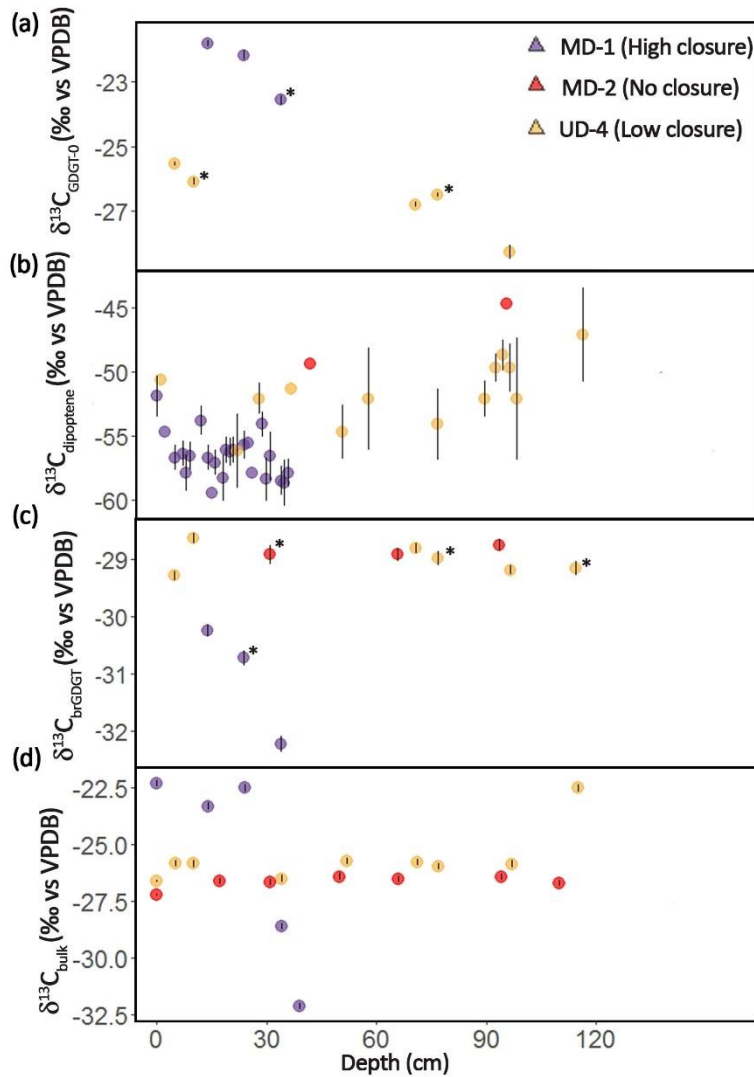
250 **3.2.1. GDGT-0 and diploptene**

251 The $\delta^{13}\text{C}$ value of GDGT-0 is ^{13}C -enriched compared with that of the brGDGT lipids, with
252 MD-1 (high closure) exhibiting higher $\delta^{13}\text{C}$ values than UD-4 (low closure, $-22.6 \pm 0.2\text{‰}$, $n =$
253 3 versus $-26.2 \pm 0.2\text{‰}$, $n = 6$, Fig. 3). In MD-1, the $\delta^{13}\text{C}$ value of GDGT-0 decreases with
254 increasing depth while it stayed constant for UD-4.

255 Most of MD-2 (no closure) samples are below detection limit for diploptene $\delta^{13}\text{C}$
256 measurements. When measurable, the $\delta^{13}\text{C}$ value of diploptene is significantly lower than that
257 of the GDGTs (Fig. 3), in average $-47.0 \pm 3.3\text{‰}$ in MD-2 ($n = 2$), $-51.6 \pm 2.5\text{‰}$ in UD-4 ($n =$
258 13) and $-56.5 \pm 1.8\text{‰}$ in MD-1 ($n = 24$). In MD-1 (high closure), diploptene is more ^{13}C -
259 enriched at the top of the cores than deeper downcore, exhibiting a trend similar to the GDGTs.
260 In UD-4 (low closure), $\delta^{13}\text{C}$ values of diploptene increase at the bottom of the core.

261 **3.2.2. BrGDGTs**

262 All branched GDGTs have been pooled for ^{13}C measurements, with 3 cm resolution. MD-2 (no
 263 closure) and UD-4 (low closure) have similar $\delta^{13}\text{C}$ values of $-29.0 \pm 0.3\text{‰}$ (Fig. 3c) (n = 9)
 264 while MD-1 (high closure) is more ^{13}C -depleted ($-31.1 \pm 0.2\text{‰}$; n = 3). In MD-1, the $\delta^{13}\text{C}$ value
 265 of the brGDGTs decreases with increasing depth while it stayed constant with depth in the
 266 other lakes (Fig. 3c).



267
 268 **Figure 3** Carbon stable isotope compositions of (a) GDGT-0, (b) diploptene (three samples
 269 could not be run in duplicate and therefore do not have error bars), (c) brGDGT, and (d) bulk
 270 TOC (Lattaud et al., submitted) in the Mackenzie delta lakes. Asterisks (*) indicate low F2/F1,
 271 and therefore $\delta^{13}\text{C}_{\text{GDGT}}$ values influenced more strongly by background carbon.

272

273 **4 Discussion**

274 **4.1. Origin of GDGTs in Mackenzie Lakes**

275 **4.1.1. iGDGT reflect in situ methane production**

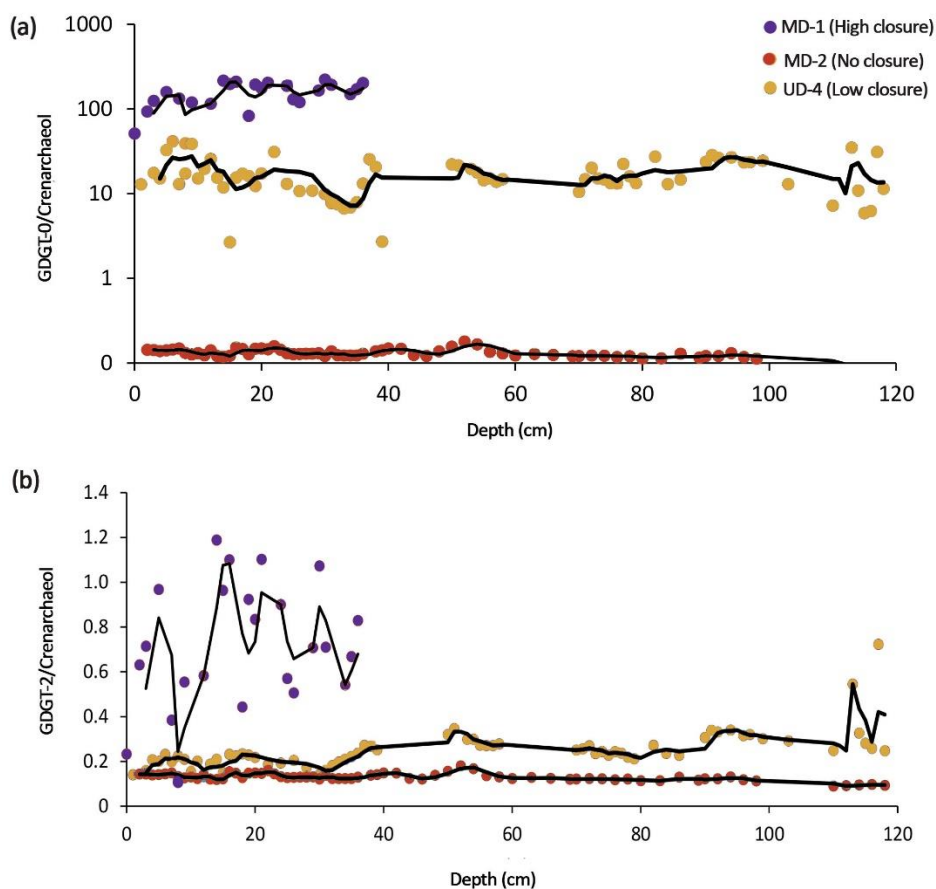
276 The distribution of the iGDGTs is dominated by GDGT-0 (Fig. 2), comprising more than 90%
277 of all iGDGTs. Previous studies have shown that the number of cyclopentane rings in GDGTs
278 from surface sediments substantially increases with increasing lake temperature (Schouten et
279 al., 2002), hence the predominance of GDGT-0 is not a surprise in arctic lakes (MAT = $-8.4 \pm$
280 1.7 °C, 1960 – 2020, Inuvik weather station). However, the absence of crenarchaeol is
281 surprising, and the observed distribution differs from those of permafrost samples of Kusch et
282 al. (2019), and more closely resembles those found in the deep anoxic regions of Lake Chala,
283 Africa (Sinninghe Damsté et al., 2009b) and Lake Rotsee, Switzerland (Naehler et al., 2014a).
284 GDGT-0 can be produced by a wide range of Archaea; Thaumarchaeota (Oger and Cario, 2013;
285 Schouten et al., 2013; Villanueva et al., 2014; Elling et al., 2017), thermophilic and mesophilic
286 Crenarchaeota, as well as in methanogens and Euryarchaeota that mediate the anaerobic
287 oxidation of methane (Koga et al., 1993; Pancost et al., 2001; Bauersachs et al., 2015). The
288 near absence of crenarchaeol in addition to the low concentration of GDGT-1 to 3 points toward
289 a precursor other than the lacustrine Thaumarchaeota, and methanogenic or methanotrophic
290 Archaea are a likely predominant source of GDGT-0 in Mackenzie delta lakes.

291 Blaga et al. (2009) proposed the ratio of GDGT-0 over crenarchaeol is an indicator of
292 methanogenesis in lakes. A value above 2 was suggested as indicative of the presence of
293 anaerobic methanogenesis, although few studies clearly demonstrated a strong correlation
294 (Naehler et al., 2014a). In the Mackenzie delta, MD-1 (high closure) has an average GDGT-
295 0/crenarchaeol ratio of 152 ± 51 while the ratios for UD-4 (low closure) and MD-2 (no closure)
296 are of 17 ± 8 and $< 1.6 \pm 0.3$, respectively (Fig. 5). These ratios for the high closure and low
297 closure lakes are much higher than those reported by Blaga et al. (2009) in European lakes, but

298 similar to Pan et al. (2016) in marine hydrothermal deposits and to some lakes such as Lake
299 Honghu (China) with low oxygen content (Dang et al., 2016) and eutrophic Lake Rotsee
300 (Switzerland) (Naeher et al., 2014b). The low values in MD-2 could indicate limited
301 methanogenesis. Biomass from high emergent macrophyte productivity in Mackenzie delta
302 lakes during summer is rapidly oxidized under the ice during winter, creating anoxia. The
303 protracted interval of water column anoxia as well as the abundance of $\text{CO}_{2(\text{aq})}$ – due to high
304 organic matter input and freezing of the lake – create an ideal habitat for anaerobic
305 methanogens in the water column or sediment-water interface. In early summer, when the lake
306 water column is oxic, these organisms could persist deeper in the sediment. Their 16S rRNA
307 genes have been detected in the water column of some lakes of the delta (Bergstresser, 2018)
308 and in the water column and sediments of other Arctic thermokarst lakes (Heslop et al., 2015;
309 Matheus Carnevali et al., 2015; Crevecoeur et al., 2016). However, Bergstresser (2018) only
310 detect few reads (one OTU linked to methanogenic Archaea), which they attributed to the use
311 of a non-specific 16S rRNA primer.

312 Several other cyclic iGDGT ratios have been defined in order to trace the presence of
313 methanotrophic archaea (Blaga et al., 2009; Zhang et al., 2011), i.e., GDGT-2 over
314 crenarchaeol and GDGT-1, -2, -3 over crenarchaeol (methane index), respectively. For the first
315 ratio, values > 0.2 points toward methanotrophy (Blaga et al., 2009), while for the methane
316 index, values > 0.5 indicate significant production of iGDGT by methanotrophic Euryarchaeota
317 (Zhang et al., 2011). For the Mackenzie delta, GDGT-2/Crenarchaeol ratios exceed the
318 threshold value for methanotrophy for MD-1 (high closure) and UD-4 (low closure) (0.7 ± 0.3
319 and 0.3 ± 0.1 , respectively), while MD-2 (no closure) fall below this threshold (Fig. 5). The
320 methane index is relatively high in the high closure lake sediments of the Mackenzie delta
321 (MD-1, 0.7 ± 0.1) in comparison with those from low and no closure lakes (MD-2 0.3 ± 0.1
322 and UD-4 0.4 ± 0.1 , respectively). Both ratios thus indicate the potential presence of

323 methanotrophic Archaea in MD-1 (high closure). The anaerobic oxidation of methane is
 324 characterised by a low energy yield (Nauhaus et al., 2002) and, so far, three communities of
 325 Euryarchaeota (ANME-1, -2, -3) were identified in consortium with sulphate-reducing bacteria
 326 (SRB) that provide electron acceptor (SO_4^{2-}). But other oxidants (e.g., Fe(III), Mn(IV)) are also
 327 plausible (e.g., Beal et al., 2009). In high closure lakes, iron and sulfate concentrations are
 328 elevated (Geeves, 2019), and anoxia and high methane concentrations could favor the presence
 329 of methanotrophic Archaea.



330
 331 **Figure 4** GDGT ratios (a) GDGT-0/crenarchaeol, (b) GDGT-2/crenarchaeol in Mackenzie
 332 delta lakes.

333
 334 We measured the carbon isotopic composition of GDGT-0 in order to assess the role of Archaea
 335 in the methane cycle in the Mackenzie River delta lakes. In low closure (UD-4) and high
 336 closure (MD-1) lakes, where GDGT-0 was present in sufficient abundance for isotopic

337 measurement, $\delta^{13}\text{C}_{\text{GDGT-0}}$ values are ^{13}C -enriched compared to brGDGTs, with higher values
338 for MD-1 ($-22.5 \pm 0.2\text{‰}$) than for UD-4 ($-26.6 \pm 0.3\text{‰}$). These compositions are similar to
339 those of the $\delta^{13}\text{C}_{\text{TOC}}$ ($-22.7 \pm 0.3\text{‰}$ and $-26.0 \pm 0.4\text{‰}$, respectively), which could point towards
340 the production by heterotrophic Archaea in the lakes although the fractionation is very small.
341 GDGT-0 could also be produced by acetoclastic or hydrogenotrophic methanogenic Archaea,
342 utilizing acetate or dissolved CO_2 as their carbon source for biosynthesis. In the latter, lipid
343 $\delta^{13}\text{C}$ values would reflect that of lake water $\text{CO}_{2(\text{aq})}$ after accounting for fractionation during
344 carbon fixation and biosynthesis. Although $\delta^{13}\text{C}_{\text{CO}_{2(\text{aq})}}$ values are not directly available for the
345 lakes examined in this study, they can be calculated from $\delta^{13}\text{C}$ values of dissolved inorganic
346 carbon (DIC) (assuming about a 10‰ fractionation between DIC and $\text{CO}_{2(\text{aq})}$ at 10 °C , Mook
347 et al., 1974). During spring to summer there is a decrease in $\delta^{13}\text{C}_{\text{DIC}}$ values due to the decrease
348 in $p\text{CO}_2$ (-7.6‰ in June to -13‰ in August for high closure lakes, Tank, 2009), which would
349 yield corresponding $\delta^{13}\text{C}_{\text{CO}_{2(\text{aq})}}$ values of ~ -17 to -23‰ . However, most methanogens are
350 expected to be productive in winter (see above) when high $p\text{CO}_2$ (due to under-ice
351 accumulation following the release by permafrost) is expected and the $\delta^{13}\text{C}_{\text{CO}_{2(\text{aq})}}$ likely ^{13}C -
352 enriched compared to summer. Unfortunately, the $\delta^{13}\text{C}_{\text{CO}_{2(\text{aq})}}$ or $\delta^{13}\text{C}_{\text{DIC}}$ values of the winter
353 lake water are not known. Methanogenesis commonly occurs in anoxic parts of lake sediments
354 and overlying waters, where the dominant mechanism in freshwater environments is via the
355 acetoclastic pathway (Whiticar et al., 1986). The latter results in a -2 to -6‰ fractionation in
356 the produced lipids, while hydrogenotrophic methanogenesis, which has also been reported in
357 cold environments, results in higher fractionation ($\Delta_{\text{substrate-lipid}} = -11$ to -20‰ , Londry et al.,
358 2008; Penning et al., 2006; Valentine et al., 2004; Whiticar et al., 1986). Furthermore,
359 methylotrophic methanogenesis would result in an even higher fractionation ($\Delta_{\text{substrate-lipid}} = -$
360 33 to -46‰). but is rarely reported in freshwater environments due to the lower availability of
361 these substrates. ^{13}C - CH_4 measurements in pore-waters of surface sediment of high closure

362 lakes suggest dominant hydrogenotrophic methanogenesis with a minor contribution from the
363 acetoclastic pathway (-80 to -50‰, Geeves, 2019), while 16S rRNA sequencing suggests a
364 larger gene copies of Archaea involved in acetoclastic methanogenesis (Bergstresser, 2018).
365 Furthermore, Bergstresser (2018) reported the presence of *Methanosaeta* (methanogenic
366 Archaea) in the top sediment (0 – 2 cm) of the Mackenzie delta lakes in winter and early spring
367 and the possibility for aerobic methanogenesis to occur in the water-column of high closure
368 lakes.

369 Our $\delta^{13}\text{C}_{\text{GDGT-0}}$ values suggest a possible contribution of GDGT-0 by non-methanogenic
370 Archaea but are also compatible with a significant contribution by acetoclastic methanogens.
371 The difference in $\delta^{13}\text{C}_{\text{GDGT-0}}$ values between the lakes likely reflects differences in $\delta^{13}\text{C}_{\text{CO}_2(\text{aq})}$
372 due to contrasting $p\text{CO}_2$ (higher for MD-1 and high closure lakes in general, Lesack et al.,
373 1998; Squires et al., 2009).

374 No methanotrophic Archaea were reported by Bergstresser (2018). This might be due to the
375 primer used in the study, but this finding is in agreement with the carbon isotopic composition
376 of GDGT-0 (Fig. 3), which is not significantly ^{13}C -depleted compared to the $\delta^{13}\text{C}_{\text{CH}_4}$.
377 Anaerobic methanotrophy is rare in freshwater environments due to low sulfate (i.e., electron
378 acceptor) concentrations. In contrast, Bergstresser (2018) detected large amounts of bacteria
379 known to mediate the aerobic oxidation of methane (i.e., MOB), which are especially abundant
380 during winter. MOB produce hopanoids that are depleted in ^{13}C compared to lipids produced
381 by photosynthetic autotrophs (e.g., sterols, *n*-alkanes; Pancost et al., 2000). In agreement with
382 this observation, we find large amount of diploptene (17 β (H), 21 β (H)-hop-22(29)-ene) in MD-
383 1 (high closure) and UD-4 sediments (low closure) with $\delta^{13}\text{C}$ values of $-51.6 \pm 2.5\text{‰}$ and -56.6
384 $\pm 1.8\text{‰}$, respectively, comparable with values reported for Alaskan Arctic thermokarst lakes
385 (Davies et al., 2016). Hence, it seems that the oxidation of methane occurs aerobically and is

386 primarily mediated by bacteria, but further studies that target the methanotrophic archaea
387 (using specific primers or biomarkers) are needed.

388

389 **4.1.2. Provenance of brGDGT lipids**

390 BrGDGTs in lake sediments can derive from the watershed, after soil erosion, and from in situ
391 production within the lake water column itself. Elucidating the source of these lipids is
392 necessary before paleoclimate information can be robustly retrieved from their distributions.

393 In a ternary plot for globally distributed soils and lakes (Fig. 2), the GDGT distribution of
394 Mackenzie lake sediments plot towards cold soils and lakes, similar to that observed in
395 Antarctic lakes (Foster et al., 2016). The dominant brGDGTs are the non-cyclopentane
396 containing pentamethylated as well as hexamethylated 5 and 6 methyl brGDGTs (IIa, IIa', IIIa
397 and IIIa', respectively; Fig. 2) which have been suggested to be indicative of in situ production
398 in lakes (Blaga et al., 2009; Tierney et al., 2010; Pearson et al., 2011; Sun et al., 2011; Shanahan
399 et al., 2013; Peterse et al., 2014; Russell et al., 2018). Tetramethylated brGDGTs Ia, Ib and Ic
400 are usually characteristic for soil input (Fig. 2, e.g., Weijers et al., 2007; Zink et al., 2016;
401 Russel et al., 2018). However, soils from cold areas such Alaska and Svalbard) and permafrost
402 soils from Siberia (Kush et al., 2019) have a higher IIIa proportion than temperate and tropical
403 soils (Weijers et al., 2007). One soil from the Mackenzie River delta has been measured
404 (Peterse et al., 2014) and has 42% IIIa + IIIa', but the analysis has been done with an older
405 protocol without differentiating 6-methyl isomers from 5-methyl isomers. Taking the pH of
406 this soil (6.5) and the associated IR value (0.49, Yang et al., 2015) into account, there is likely
407 equal proportions of IIIa and IIIa' in this soil sample, which differs from the lake samples (Fig.
408 2). Furthermore, the 5,6-methyl brGDGT IIIa'' in UD-4 sediments (low-closure lake, Fig. 2)
409 indicates the presence of in situ production, as this compound was exclusively reported from

410 lake sediments and water column suspended particulate matter and is always below detection
411 limit in soils (De Jonge et al., 2014b; Weber et al., 2015, 2018; Martin et al., 2019).

412 The BIT index is consistently above 0.9 for the three lakes (0.99 in soil, Peterse et al., 2014),
413 but these high values in the lakes likely reflect the low crenarchaeol concentration (Fig. 2)
414 rather than an indicator of soil input. The IIIa/IIa ratio (Xiao et al., 2016; Martin et al., 2019)
415 is 1.6 ± 0.4 for UD-4, 1.5 ± 0.2 for MD-2 and 1.4 ± 0.3 for MD-1, which also points toward a
416 lacustrine in situ production (the reported threshold is > 0.9 for in situ aquatic production, in
417 one soil of the Mackenzie region it is 1.2, Peterse et al., 2014). The Mackenzie River transports
418 large quantities of soil-derived organic matter (Vonk et al., 2019), and is therefore a potential
419 source of soil-derived brGDGTs, especially to the no-closure lakes. However, the distribution
420 of brGDGTs in Mackenzie River SPM differs from that in lakes with IIa (IIa + IIa') and IIIa
421 (IIIa = 15% and IIIa' = 19%) as main brGDGTs (34% each, Peterse et al., 2014) and IIIa/IIa
422 equal to 1.0 ± 0.1 ($n = 6$; Peterse et al., 2014). Furthermore, as Peterse et al. (2014) noted, the
423 concentration of brGDGTs in the lakes (total brGDGTs $19 - 33 \mu\text{g g}_{\text{TOC}}^{-1}$) are significantly
424 higher than in the Mackenzie River (total brGDGTs $0.4 - 3.9 \mu\text{g g}_{\text{TOC}}^{-1}$) where soil brGDGTs
425 could originate. In conclusion, the brGDGT distribution indicates a dominant in situ lacustrine
426 production in all studied lakes, irrespective of their degree of closure, and with no apparent
427 changes in provenance downcore.

428 The production of IIIa'' has been previously found to be confined to the anoxic part of the
429 water column of Lake Lugano and Hinterburg, Switzerland (Weber et al., 2015, 2018). It is
430 also reported in sediments from Lake St Front, France (Martin et al., 2019). In the Mackenzie
431 lake sediments it is only found in lake UD-4 (low closure). Mackenzie delta lake bottom waters
432 experience anoxia during the winter season when ice effectively seals the lakes and large
433 amounts of organic matter is respired (Squires et al., 2009). However, the other studied lakes
434 also experience anoxia in winter yet do not show any IIIa'' production, suggesting that this

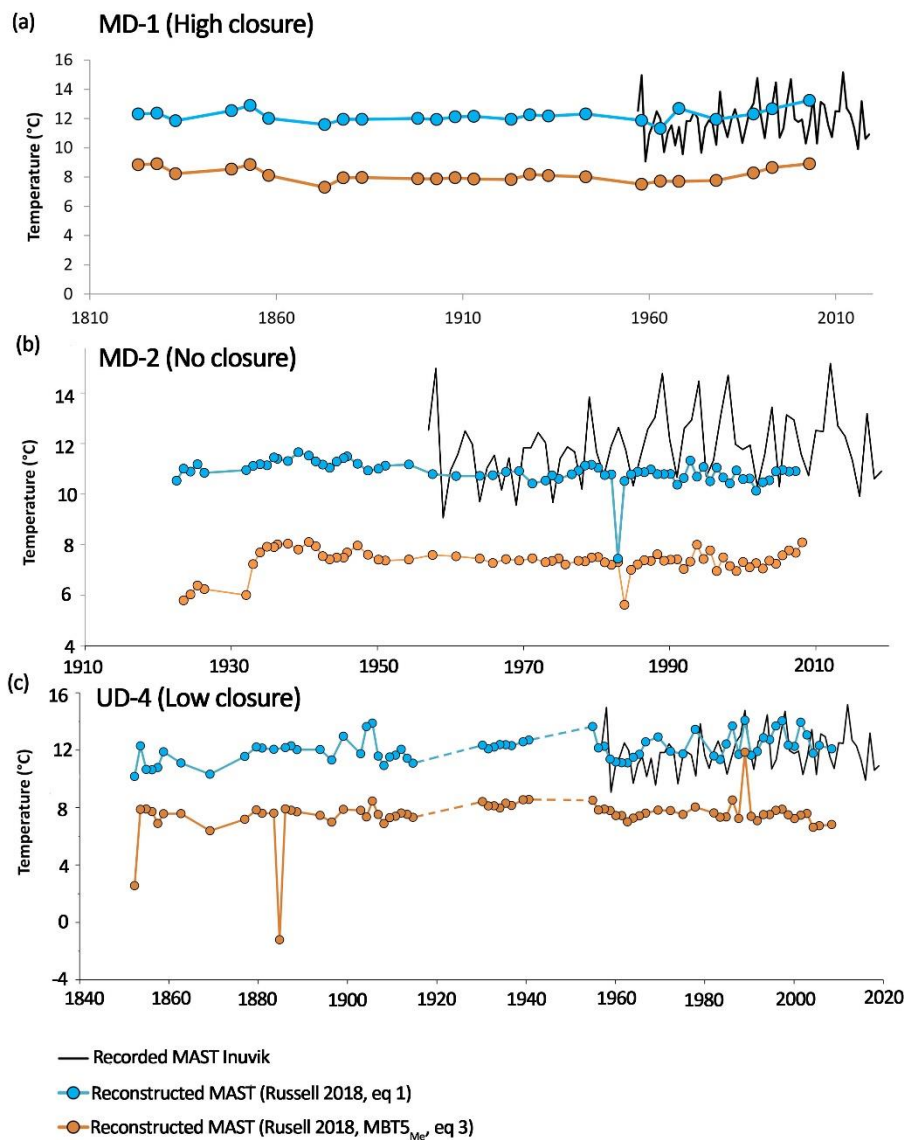
435 GDGT it is not a specific marker for anoxia. IIIb^X, a brGDGT with an unknown structure, has
436 not been reported before and is only present in lake MD-1, whereas IIIc^X, another brGDGT
437 with unknown structure, is found in lakes UD-4 and MD-2 but has not been reported in other
438 lakes (Fig. 2). As the proportion of IIIb isomers and IIIc isomers increase with increasing pH,
439 and MD-1 has a higher pH than the other lakes, the presence of IIIb^X could tentatively be
440 attributed to increased pH. However, this inference, together with the curious presence of IIIc^X
441 in MD-2 and UD-4, requires more study, in particular through analysis of SPM from the lakes.

442
443 The $\delta^{13}\text{C}$ values of brGDGTs can shed light on the metabolism of brGDGT producers (Naehrer
444 et al., 2014; Weber et al., 2015, 2018). The values found in lake UD-4 (low closure) and MD-
445 2 (no closure) are similar and constant over the length of each cores ($-29.0 \pm 0.2\text{‰}$ and -28.9
446 $\pm 0.2\text{‰}$, respectively) and also present a systematic 3‰ offset with $\delta^{13}\text{C}_{\text{TOC}}$ ($-26.0 \pm 0.4\text{‰}$ and
447 $-26.6 \pm 0.4\text{‰}$, Lattaud et al., submitted) as was observed in lake SPM before by Weber et al.
448 (2018). The $\approx 3\text{‰}$ difference between the brGDGTs and the TOC is consistent with the
449 heterotrophic metabolism of Acidobacteria (Kielak et al., 2016), with the breakdown and
450 assimilation of particulate organic carbon in the water column and surface sediments. For the
451 upper part of the MD-1 (high closure) core, the $\delta^{13}\text{C}_{\text{TOC}}$ is significantly higher ($-22.8 \pm 0.3\text{‰}$,
452 > 22 cm) while the $\delta^{13}\text{C}_{\text{brGDGT}}$ is significantly lower ($-31.1 \pm 0.2\text{‰}$). In contrast, $\delta^{13}\text{C}_{\text{TOC}}$ values
453 in the lower part of MD-1 were markedly lower ($-27.9 \pm 0.3\text{‰}$) while the $\delta^{13}\text{C}_{\text{brGDGT}}$ values
454 were similar to those in the upper part ($-32.7 \pm 0.3\text{‰}$). The top part of the sediment core is a
455 mix of labile carbon (macrophyte-derived and MOB-derived), as indicated by younger TOC
456 ^{14}C ages while deeper in the core only the refractory, pre-aged OC remain (mainly terrestrial
457 higher-plant-derived, Lattaud et al., submitted). This suggests that the lacustrine brGDGT-
458 producers consume labile organic carbon such as a mix of MOB-derived and macrophyte-
459 derived. In no-closure and low-closure lakes characterized by macrophyte production (Squires

460 and Lesack, 2002) and less MOB-derived OM, terrestrial plant-derived OM may serve as a
461 more important carbon source for brGDGT producers.

462 Hence, the large difference ($\sim 9\%$) between $\delta^{13}\text{C}_{\text{GDGT}}$ and $\delta^{13}\text{C}_{\text{TOC}}$ in the upper part of the core
463 from MD-1 points toward the heterotrophic consumption by brGDGT producers of labile, ^{13}C -
464 depleted MOB-derived organic matter instead of more refractory ^{13}C -enriched compounds.

465 While in MD-2 and UD-4, brGDGT producers are likely feeding (using fermentation) on more
466 refractory terrestrial-plant derived OM due to the depletion of labile compounds.



467

468 **Figure 5** Temperature reconstruction using brGDGTs in (a) MD-1 (high closure), (b) MD-2

469 (no closure) and (c) UD-4 (low closure). Mean summer temperature at Inuvik, GDGT-

470 reconstructed summer temperature using equation 1 (Russell et al., 2018) and using equation 3
471 (Russell et al., 2018).

472

473 **4.2. Environmental reconstruction using brGDGTs**

474 **4.2.1. Calculation of GDGT-based temperatures**

475 Several temperature calibrations exist for lakes, many of which are lake-specific (e.g., Foster
476 et al., 2016; Pearson et al., 2011; Sun et al., 2011; Zink et al., 2016), hindering their use in other
477 locations. The Mackenzie delta is characterized by low annual air temperatures (-8.4 ± 1.7 °C
478 average of the last 60 years at Inuvik weather station) but comparably high summer
479 temperatures (11.9 ± 1.4 °C average of the last 60 years at Inuvik weather station), and the
480 lakes of the delta are only free of ice from June (freshet) to late September. A few calibrations
481 have been performed in the high Arctic (Shanahan et al., 2013; Colcord et al., 2015), but none
482 of these are based on the full suite of 15 brGDGTs (see appendix), owing to changes in the
483 analytical protocol. We therefore adopted the same approach as Shanahan et al. (2013), who
484 used a global lake calibration. We use the multivariate regression that Russell et al. (2018)
485 propose ([Eq. 1] RSME 2.14 °C) based on a set of African lake surface sediments. In addition
486 we also calculate the MBT'_{5ME} index as defined by De Jonge et al. (2014b) [Eq. 2] and apply
487 the calibrations calculated by Russell et al. (2018) ([Eq. 3], RSME = 2.43 °C). We interpret the
488 reconstructed temperatures as mean annual summer temperatures since it is likely, although
489 not proven, that the brGDGTs are mainly produced when the region is free of ice (Shanahan et
490 al., 2013).

491

$$492 \text{ MAST} = 23.81 - 31.02 \times IIIa - 41.91 \times IIb - 51.59 \times IIb' - 24.70 \times IIa + 68.80 \times$$
$$493 \text{ Ib} \tag{1}$$

$$494 \text{ MBT}'_{5Me} = \frac{Ia+Ib+Ic}{Ia+Ib+Ic+IIa+IIb+IIc+IIIa} \tag{2}$$

495 $MAST = -1.21 + 32.42 \times MBT'_{5Me}$ (3)

496

497 The absolute reconstructed temperatures using [Eq. 1] are in the range of those recorded in
498 summer at Inuvik during the last 60 years, supporting the validity of this calibration, while
499 those reconstructed by [Eq. 3] are lower (~ 4 °C lower than recorded temperatures, Fig. 5). The
500 reconstructed temperatures using [Eq. 1] and [Eq. 3] present the same pattern for MD-1 and
501 UD-4 but differ in the bottom part of MD-2. The latter could indicate that [Eq. 2] is influenced
502 by parameters other than temperature, such as oxygen concentration and pH changes (see
503 below). Furthermore, we note that MBT'_{5Me} is, on average, increasing with decreasing
504 connectivity to the river (Fig. 6), implying that this ratio is not only controlled by variations in
505 temperature.

506 In MD-1 there is a slight increase (+1 °C) in MAST over the record [Eq. 1], but UD-4 present
507 more variation than MD-1 which could reflect the slow sedimentation in MD-1 that buffers
508 large changes in temperature. In UD-4 the most recent part of the record seems to capture the
509 yearly variability recorded in the instrumental record [Eq. 1]. This absence of warming reflects
510 the stability of the summer temperatures in the region, and equation [Eq. 1] seems to be better
511 at capturing yearly variability in temperature. Hence, equation [Eq. 1] is recommended in the
512 Mackenzie delta lakes to reconstruct summer air temperature.

513

514 **4.2.2. BrGDGTs as indicators of lake hydrology and connectivity**

515 The three lakes studied differ with respect to their connectivity to the river, as well as their size
516 and depth. For example, MD-2 (no closure) is the largest and deepest lake, while UD-4 (low
517 closure) and MD-1 (high closure) have a rather small area and are quite shallow (~ 1 m deep).
518 Due to this variation in connectivity their nutrient content and chemical properties are also
519 expected to be different. The mean annual pH of the lakes is similar but can significantly vary

520 over the course of the year, being as high as ~10 in late summer in high closure lakes while
 521 remaining at ~7.8 in no closure lakes (similar to the Mackenzie River, Tank et al., 2008, 2009).
 522 A principal component analysis (PCA, Fig. S1), performed for each lake using the fractional
 523 abundance of all 15 brGDGT compounds, reveals that in MD-2 (no closure lake) and UD-4
 524 (low closure), the principal component 1 (PC1) (explaining 68% and 52% of the variance,
 525 respectively) is represented by IIIa' and IIIa'', which may reflect anoxic conditions (Weber et
 526 al., 2018), while PC2 (explaining 14% and 25% of the variance, respectively) is represented by
 527 IIIa which likely reflects a temperature control (as it is included in [Eq. 1] and [Eq. 2]). In MD-
 528 1, the main sources of variation differ, with IIa' and IIIa having a high (and opposite) loading
 529 on PC1 (explaining 58% of the variance) and IIIa' on PC2 (explaining 33% of the variance).
 530 Hence, both temperature and oxygen availability seem to exert significant influence on the
 531 distribution of brGDGTs in Mackenzie lakes. Weber et al. (2018) observed more brGDGT
 532 isomers (6-methyl and 5,6-methyl) as well as a stronger increase in IIIa' than in IIa' in the
 533 anoxic part of the water column of Lake Lugano. To assess this, the isomer ratios (IR) have
 534 been calculated for the GDGT-IIIa and the GDGT-IIa (IR_{IIIa} [Eq. 5] and IR_{IIa} [Eq. 6]):

$$536 \quad IR_{IIIa} = \frac{IIIa'}{IIIa' + IIIa} \quad (5)$$

$$537 \quad IR_{IIa} = \frac{IIa'}{IIa' + IIa} \quad (6)$$

538
 539 Overall, there is an increase in average downcore IR values with decreased lake connection
 540 (significant for IR_{IIa} between all lakes and significant for IR_{IIIa} between NC and HC and LC
 541 and HC, t-test < 0.05) with the Mackenzie River (Fig. 6), in agreement with longer anoxic
 542 conditions in high closure lakes. This control of the river connectivity also influences the
 543 MBT'_{5Me} values, which on average show an increase (significant between LC to HC and NC
 544 to HC, t-test < 0.05) with decreasing connectivity (Fig. 6).

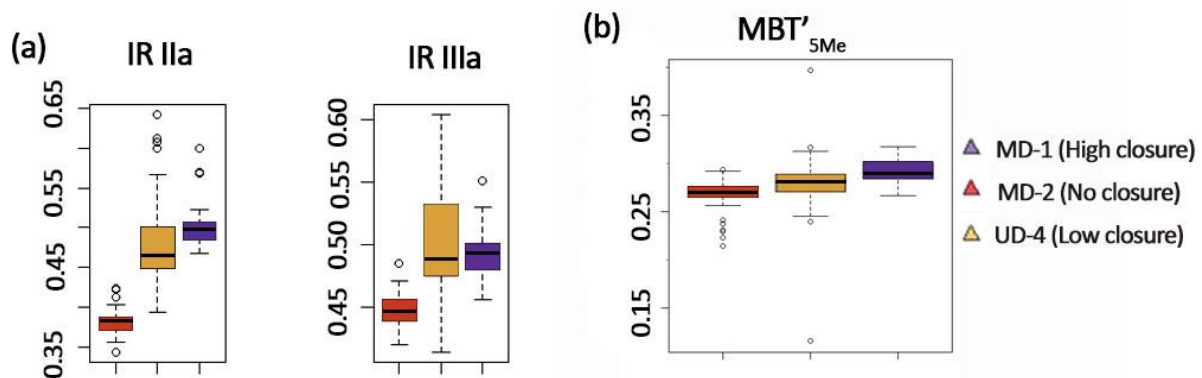
545 In prior studies, brGDGTs have been linked to other environmental parameters than
 546 temperature, such as variation in pH (e.g. De Jonge et al., 2014b), with the CBT_{5Me} allowing
 547 for the reconstruction of pH in soils and lakes ([Eq. 4] and [Eq. 5]):

$$549 \quad CBT_{5Me} = \frac{Ib+IIb}{Ib+IIb+Ia+IIa} \quad (4)$$

$$550 \quad pH = 7.84 - 1.73 \times CBT_{5Me} \quad (5)$$

551

552 The reconstructed pH in all lakes is similar (6.8 ± 0.1 for MD-2 and UD-4, and 7.0 ± 0.1 for
 553 MD-1) and does not vary down core (data not shown). This seems unlikely given the large
 554 variability in pH between the lakes. Hence, CBT_{5Me} does not appear to reflect pH variation in
 555 the Mackenzie delta lakes and brGDGTs are likely controlled by other environmental
 556 parameters such as redox properties but also possibly the trophic state of the lakes.



557

558 **Figure 6** brGDGT ratios in link with the river connection with (a) isomer ratios of GDGT-IIIa
 559 and GDGT-IIa and (b) MBT'_{5Me} .

560

561 5 Conclusion

562 In a step towards assessment of the effects of recent warming in the Canadian arctic on aquatic
 563 ecosystems of the region, and potential feedbacks with respect to greenhouse gas emissions,

564 we have investigated microbial lipid (GDGT) signatures in sediments from three Mackenzie
565 River delta lakes. The iGDGT compositions are dominated by GDGT-0, a potential marker for
566 the presence of methanogens, in agreement with the quasi absence of crenarchaeol, and
567 corresponding ^{13}C -signatures are compatible with an acetoclastic methanogenic source along
568 with a significant production by heterotrophic archaea. The abundance and ^{13}C -depleted
569 signature of diploptene indicates methane consumption via bacterial aerobic oxidation rather
570 than anaerobic oxidation by Archaea. BrGDGT composition reveals a predominant “cold”
571 signature that seems to be dominated by in situ lacustrine production of hexamethylated and
572 pentamethylated brGDGTs, in agreement with the presence of the uncommon IIIa[’], IIIb^X and
573 IIIc^X GDGT. Temperature reconstructions using brGDGTs suggest a near stable summer air
574 temperature for the last century, in agreement with recent instrumental records (> 1960 C.E.).
575 A strong control of the lake connectivity on the brGDGT distributions is evident, apparently
576 linked with the oxygen content of the lakes.

577

578 **Competing interests**

579 The authors declare that they have no conflict of interest.

580

581 **Acknowledgements**

582 We thank members of the sampling team for collecting the sediment cores from the Mackenzie
583 River lakes, Jorien Vonk for slicing MD-2 and UD-4, and Liviu Giosan for providing core MD-
584 1. Daniel Montlucon is thanked for laboratory support, Steward Bishop and the Climate
585 Geology group are thanked for instrument access. J.L. was funded by a Rubicon grant
586 [019.183EN.002] from NWO, Netherlands Organization for scientific research.

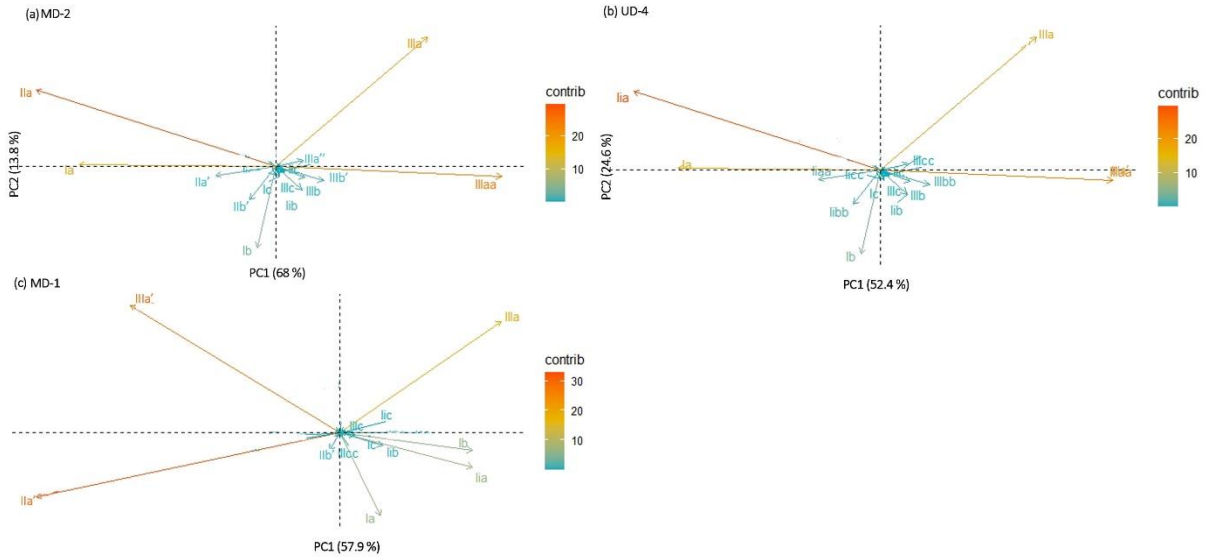
587

588 **Data availability**

589 Data from this study will be available from the PANGEA repository (doi:).

590

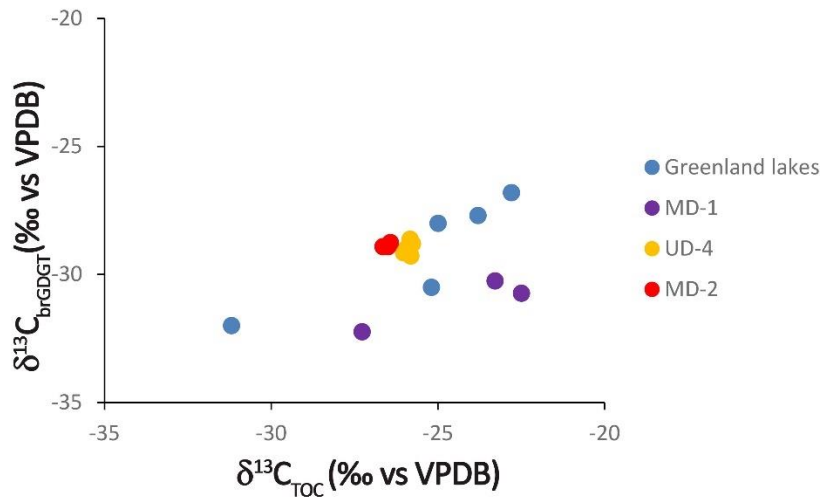
591 **Supplement**



592

593 **Figure S1:** Principal component analysis of brGDGT on (a) MD-2 (no closure), (b) UD-4 (low

594 closure) and (c) MD-1 (high closure).



595

596 **Figure S2:** Carbon stable isotope compositions of brGDGT relatively to the carbon stable

597 isotope compositions of the bulk organic matter (Lattaud et al., submitted). Data from Colcord

598 et al. (2017) are represented for comparison.

599

600 **References**

- 601 Bauersachs, T., Weidenbach, K., Schmitz, R.A., Schwark, L., 2015. Distribution of glycerol
602 ether lipids in halophilic, methanogenic and hyperthermophilic archaea. *Organic*
603 *Geochemistry* 83–84, 101–108.
- 604 Beal, E.J., House, C.H., Orphan, V.J., 2009. Manganese- and Iron-Dependent Marine Methane
605 Oxidation 311.
- 606 Bergstresser, M., 2018. Composition of aquatic microbial communities and their relation to
607 water-column methane cycling among Mackenzie Delta lakes , western Canadian Arctic
608 by.
- 609 Blaga, C.I., Reichart, G.J., Heiri, O., Sinninghe Damsté, J.S., 2009. Tetraether membrane lipid
610 distributions in water-column particulate matter and sediments: A study of 47 European
611 lakes along a north-south transect. *Journal of Paleolimnology* 41, 523–540.
- 612 Canada, G. of, n.d. Environmental and climate change Canada [WWW Document]. URL
613 https://climate.weather.gc.ca/historical_data/search_historic_data_e.html
- 614 Carrie, J., Sanei, H., Goodarzi, F., Stern, G., Wang, F., 2009. Characterization of organic matter
615 in surface sediments of the Mackenzie River Basin, Canada. *International Journal of Coal*
616 *Geology* 77, 416–423.
- 617 Carson, M.A., Jasper, J.N., Conly, F.M., 1998. Magnitude and Sources of Sediment Input to
618 the Mackenzie Delta, Northwest Territories. *Arctic* 51, 116–124.
- 619 Colcord, D.E., Cadieux, S.B., Brassell, S.C., Castañeda, I.S., Pratt, L.M., White, J.R., 2015.
620 Assessment of branched GDGTs as temperature proxies in sedimentary records from
621 several small lakes in southwestern Greenland. *Organic Geochemistry* 82, 33–41.
- 622 Colcord, D.E., Pearson, A., Brassell, S.C., 2017. Carbon isotopic composition of intact
623 branched GDGT core lipids in Greenland lake sediments and soils. *Organic Geochemistry*
624 110, 25–32.

625 Crevecoeur, S., Vincent, W.F., Lovejoy, C., 2016. Environmental selection of planktonic
626 methanogens in permafrost thaw ponds. *Scientific Reports* 6, 1–10.

627 Dang, X.Y., Xue, J.T., Yang, H., Xie, S.C., 2016. Environmental impacts on the distribution
628 of microbial tetraether lipids in Chinese lakes with contrasting pH: Implications for
629 lacustrine paleoenvironmental reconstructions. *Science China Earth Sciences* 59, 939–
630 950.

631 Davies, K.L., Pancost, R.D., Edwards, M.E., Walter Anthony, K.M., Langdon, P.G., Torres,
632 L.C., 2016. Diploptene $\delta^{13}\text{C}$ values from contemporary thermokarst lake sediments show
633 complex spatial variation. *Biogeosciences* 13, 2611–2621.

634 De Jonge, C., Hopmans, E.C., Zell, C.I., Kim, J.-H.H., Schouten, S., Sinninghe Damsté, J.S.,
635 Jonge, C. De, Hopmans, E.C., Zell, C.I., Kim, J.-H.H., Schouten, S., Damsté, J.S.S.,
636 2014a. Occurrence and abundance of 6-methyl branched glycerol dialkyl glycerol
637 tetraethers in soils: implications for palaeoclimate reconstruction. *Geochimica et*
638 *Cosmochimica Acta* 141, 97–112.

639 De Jonge, C., Stadnitskaia, A., Hopmans, E.C., Cherkashov, G., Fedotov, A., Sinninghe
640 Damsté, J.S., 2014b. In situ produced branched glycerol dialkyl glycerol tetraethers in
641 suspended particulate matter from the Yenisei River, Eastern Siberia. *Geochimica et*
642 *Cosmochimica Acta* 125, 476–491.

643 Drenzek, N.J., Montluçon, D.B., Yunker, M.B., Macdonald, R.W., Eglinton, T.I., 2007.
644 Constraints on the origin of sedimentary organic carbon in the Beaufort Sea from coupled
645 molecular ^{13}C and ^{14}C measurements. *Marine Chemistry* 103, 146–162.

646 Droppo, L.G., Jeffries, D., Jaskot, C., Backus, S., 1998. The Prevalence of Freshwater
647 Flocculation in Cold Regions : A Case Study from the Mackenzie River Delta , Northwest
648 Territories , Canada Author (s): I . G . Droppo , D . Jeffries , C . Jaskot and S . Backus
649 Published by : Arctic Institute of North Ameri 51, 155–164.

650 Dugerdil, L., Joannin, S., Peyron, O., Jouffroy-Bapicot, I., Vanni re, B., Boldgiv, B., M not,
651 G., 2020. Climate reconstructions based on GDGTs and pollen surface datasets from
652 Mongolia and Siberia: Calibrations and applicability to extremely dry and cold
653 environments. *Biogeosciences Discussions* 1–35.

654 Elling, F.J., K nneke, M., Nicol, G.W., Stieglmeier, M., Bayer, B., Spieck, E., de la Torre,
655 J.R., Becker, K.W., Thomm, M., Prosser, J.I., Herndl, G.J., Schleper, C., Hinrichs, K.U.,
656 2017. Chemotaxonomic characterisation of the thaumarchaeal lipidome. *Environmental*
657 *Microbiology* 19, 2681–2700.

658 Emmerton, C.A., Lesack, L.F.W., Marsh, P., 2007. Lake abundance, potential water storage,
659 and habitat distribution in the Mackenzie River Delta, western Canadian Arctic. *Water*
660 *Resources Research* 43, 1–14.

661 Foster, L.C., Pearson, E.J., Juggins, S., Hodgson, D.A., Saunders, K.M., Verleyen, E., Roberts,
662 S.J., 2016. Development of a regional glycerol dialkyl glycerol tetraether (GDGT)-
663 temperature calibration for Antarctic and sub-Antarctic lakes. *Earth and Planetary Science*
664 *Letters* 433, 370–379.

665 Geeves, K.A., 2019. Carbon quality and quantity in lake sediments and their relationship with
666 pore-water and lake-water methane among lakes of the Mackenzie River Delta , Western
667 Canadian Arctic by.

668 Gies, H., Hagedorn, F., Lupker, M., Montlu on, D., Haghypour, N., Voort, S. Van Der,
669 Eglinton, T.I., 2020. Millennial-age GDGTs in forested mineral soils : 14 C-based
670 evidence for stabilization of microbial necromass. *Biogeosciences Discussions* 1–26.

671 Harning, D.J., Curtin, L., Geirsd ttir,  ., D’Andrea, W.J., Miller, G.H., Sep lveda, J., 2020.
672 Lipid Biomarkers Quantify Holocene Summer Temperature and Ice Cap Sensitivity in
673 Icelandic Lakes. *Geophysical Research Letters* 47, 0–3.

674 Heslop, J.K., Walter Anthony, K.M., Sepulveda-Jauregui, A., Martinez-Cruz, K., Bondurant,

675 A., Grosse, G., Jones, M.C., 2015. Thermokarst lake methanogenesis along a complete
676 talik profile. *Biogeosciences* 12, 4317–4331.

677 Hopmans, E.C., Schouten, S., Sinninghe Damsté, J.S., 2016. The effect of improved
678 chromatography on GDGT-based palaeoproxies. *Organic Geochemistry* 93, 1–6.

679 Hopmans, E.C., Weijers, J.W.H., Schefuß, E., Herfort, L., Sinninghe Damsté, J.S., Schouten,
680 S., 2004. A novel proxy for terrestrial organic matter in sediments based on branched and
681 isoprenoid tetraether lipids. *Earth and Planetary Science Letters* 224, 107–116.

682 Huguet, C., Kim, J.-H., Damsté, J.S.S., Schouten, S., 2006. Reconstruction of sea surface
683 temperature variations in the Arabian Sea over the last 23 kyr using organic proxies
684 (TEX₈₆ and U₃₇^{K'}). *Paleoceanography* 21. doi:10.1029/2005pa001215

685 Kielak, A.M., Barreto, C.C., Kowalchuk, G.A., van Veen, J.A., Kuramae, E.E., 2016. The
686 ecology of Acidobacteria: Moving beyond genes and genomes. *Frontiers in Microbiology*
687 7, 1–16.

688 Koga, Y., Akagawa-Matsushita, M., Ohga, M., Nishihara, M., 1993. Taxonomic Significance
689 of the Distribution of Component Parts of Polar Ether Lipids in Methanogens. *Systematic
690 and applied microbiology* 16, 342–351.

691 Kusch, S., Winterfeld, M., Mollenhauer, G., Höfle, S.T., Schirrmeister, L., Schwamborn, G.,
692 Rethemeyer, J., 2019. Glycerol dialkyl glycerol tetraethers (GDGTs) in high latitude
693 Siberian permafrost: Diversity, environmental controls, and implications for proxy
694 applications. *Organic Geochemistry* 136, 103888.

695 Lesack, L.F.W., Marsh, P., 2007. Lengthening plus shortening of river-to-lake connection
696 times in the Mackenzie River Delta respectively via two global change mechanisms along
697 the arctic coast. *Geophysical Research Letters* 34, 1–6.

698 Lesack, L.F.W., Marsh, P., 2010. River-to-lake connectivities, water renewal, and aquatic
699 habitat diversity in the Mackenzie River Delta. *Water Resources Research* 46, 1–16.

700 Lesack, L.F.W., Marsh, P., Hecky, R.E., 1998. Spatial and temporal dynamics of major solute
701 chemistry among Mackenzie Delta lakes. *Limnology and Oceanography* 43, 1530–1543.

702 Londry, K.L., Dawson, K.G., Grover, H.D., Summons, R.E., Bradley, A.S., 2008. Stable
703 carbon isotope fractionation between substrates and products of *Methanosarcina barkeri*.
704 *Organic Geochemistry* 39, 608–621.

705 Loomis, S.E., Russell, J.M., Ladd, B., Street-Perrott, F.A., Sinninghe Damsté, J.S., 2012.
706 Calibration and application of the branched GDGT temperature proxy on East African
707 lake sediments. *Earth and Planetary Science Letters* 357–358, 277–288.

708 Mackay, J.R., 1963. The Mackenzie Delta area, N.W.T. Canada.

709 Martin, C., Ménot, G., Thouveny, N., Davtian, N., Andrieu-Ponel, V., Reille, M., Bard, E.,
710 2019. Impact of human activities and vegetation changes on the tetraether sources in Lake
711 St Front (Massif Central, France). *Organic Geochemistry* 135, 38–52.

712 Martin, C., Ménot, G., Thouveny, N., Peyron, O., Andrieu-Ponel, V., Montade, V., Davtian,
713 N., Reille, M., Bard, E., 2020. Early Holocene Thermal Maximum recorded by branched
714 tetraethers and pollen in Western Europe (Massif Central, France). *Quaternary Science*
715 *Reviews* 228. doi:10.1016/j.quascirev.2019.106109

716 Matheus Carnevali, P.B., Rohrsen, M., Williams, M.R., Michaud, A.B., Adams, H., Berisford,
717 D., Love, G.D., Priscu, J.C., Rassuchine, O., Hand, K.P., Murray, A.E., 2015. Methane
718 sources in arctic thermokarst lake sediments on the North Slope of Alaska. *Geobiology*
719 13, 181–197.

720 Mook, W.G., Bommerson, J.C., Staverman, W.H., 1974. Carbon isotope fractionation between
721 dissolved bicarbonate and gaseous carbon dioxide. *Earth and Planetary Science Letters*
722 22, 169–176.

723 Naeher, S., Niemann, H., Peterse, F., Smittenberg, R.H., Zigah, P.K., Schubert, C.J., 2014a.
724 Tracing the methane cycle with lipid biomarkers in Lake Rotsee (Switzerland). *Organic*

725 Geochemistry 66, 174–181.

726 Naeher, S., Peterse, F., Smittenberg, R.H., Niemann, H., Zigah, P.K., Schubert, C.J., 2014b.

727 Sources of glycerol dialkyl glycerol tetraethers (GDGTs) in catchment soils, water column

728 and sediments of Lake Rotsee (Switzerland) - Implications for the application of GDGT-

729 based proxies for lakes. *Organic Geochemistry* 66, 164–173.

730 Nauhaus, K., Boetius, A., Krüger, M., Widdel, F., 2002. In vitro demonstration of anaerobic

731 oxidation of methane coupled to sulphate reduction in sediment from a marine gas hydrate

732 area. *Environmental Microbiology* 4, 296–305.

733 Oger, P.M., Cario, A., 2013. Adaptation of the membrane in Archaea. *Biophysical Chemistry*

734 183, 42–56.

735 Pan, A., Yang, Q., Zhou, H., Ji, F., Wang, H., Pancost, R.D., 2016. A diagnostic GDGT

736 signature for the impact of hydrothermal activity on surface deposits at the Southwest

737 Indian Ridge. *Organic Geochemistry* 99, 90–101.

738 Pancost, R.D., Hopmans, E.C., Sinninghe Damsté, J.S., 2001. Archaeal lipids in mediterranean

739 cold seeps: Molecular proxies for anaerobic methane oxidation. *Geochimica et*

740 *Cosmochimica Acta* 65, 1611–1627.

741 Pancost, R.D., Sinninghe Damsté, J.S., De Lint, S., Van Der Maarel, M.J.E.C., Gottschal, J.C.,

742 2000. Biomarker evidence for widespread anaerobic methane oxidation in Mediterranean

743 sediments by a consortium of methanogenic archaea and bacteria. *Applied and*

744 *Environmental Microbiology* 66, 1126–1132.

745 Pearson, A., Hurley, S.J., Walter, S.R.S., Kusch, S., Lichtin, S., Zhang, Y.G., 2016. Stable

746 carbon isotope ratios of intact GDGTs indicate heterogeneous sources to marine

747 sediments. *Geochimica et Cosmochimica Acta* 181, 18–35.

748 Pearson, E.J., Juggins, S., Talbot, H.M., Weckström, J., Rosén, P., Ryves, D.B., Roberts, S.J.,

749 Schmidt, R., 2011. A lacustrine GDGT-temperature calibration from the Scandinavian

750 Arctic to Antarctic: Renewed potential for the application of GDGT-paleothermometry in
751 lakes. *Geochimica et Cosmochimica Acta* 75, 6225–6238.

752 Penning, H., Claus, P., Casper, P., Conrad, R., 2006. Carbon isotope fractionation during
753 acetoclastic methanogenesis by *Methanosaeta concilii* in culture and a lake sediment.
754 *Applied and Environmental Microbiology* 72, 5648–5652.

755 Peterse, F., van der Meer, J., Schouten, S., Weijers, J.W.H., Fierer, N., Jackson, R.B., Kim,
756 J.H., Sinninghe Damsté, J.S., 2012. Revised calibration of the MBT-CBT
757 paleotemperature proxy based on branched tetraether membrane lipids in surface soils.
758 *Geochimica et Cosmochimica Acta* 96, 215–229.

759 Peterse, F., Vonk, J.E., Holmes, R.M., Giosan, L., Zimov, N., Eglinton, T.I., 2014. Branched
760 glycerol dialkyl glycerol tetraethers in Arctic lake sediments: Sources and implications for
761 paleothermometry at high latitudes. *Journal of Geophysical Research: Biogeosciences*
762 119, 1738–1754.

763 Russell, J.M., Hopmans, E.C., Loomis, S.E., Liang, J., Sinninghe Damsté, J.S., 2018.
764 Distributions of 5- and 6-methyl branched glycerol dialkyl glycerol tetraethers
765 (brGDGTs) in East African lake sediment: Effects of temperature, pH, and new lacustrine
766 paleotemperature calibrations. *Organic Geochemistry* 117, 56–69.

767 Schouten, S., Hopmans, E.C., Damsté, E.S.J.S.S., 2002. Distributional variations in marine
768 crenarchaeotal membrane lipids: a new tool for reconstructing ancient sea water
769 temperatures? *Earth and Planetary Science Letters* 204, 265–274.

770 Schouten, S., Hopmans, E.C., Damsté, J.S.S., Sinninghe Damsté, J.S., 2013. The organic
771 geochemistry of glycerol dialkyl glycerol tetraether lipids: A review. *Organic*
772 *Geochemistry* 54, 19–61.

773 Sessions, A.L., Sylva, S.P., Hayes, J.M., 2005. Moving-Wire Device for Carbon Isotopic
774 Analyses of Nanogram Quantities of Nonvolatile Organic Carbon. *Analytical Chemistry*

775 77, 6519–6527.

776 Shanahan, T.M., Hughen, K.A., Van Mooy, B.A.S., 2013. Temperature sensitivity of branched
777 and isoprenoid GDGTs in Arctic lakes. *Organic Geochemistry* 64, 119–128.

778 Sinninghe Damsté, J.S., 2016. Spatial heterogeneity of sources of branched tetraethers in shelf
779 systems: The geochemistry of tetraethers in the Berau River delta (Kalimantan,
780 Indonesia). *Geochimica et Cosmochimica Acta* 186, 13–31.

781 Sinninghe Damsté, J.S., Ossebaar, J., Abbas, B., Schouten, S., Verschuren, D., 2009. Fluxes
782 and distribution of tetraether lipids in an equatorial African lake: Constraints on the
783 application of the TEX₈₆ palaeothermometer and BIT index in lacustrine settings.
784 *Geochimica et Cosmochimica Acta* 73, 4232–4249.

785 Sinninghe Damsté, J.S., Rijpstra, W.I.C., Foesel, B.U., Huber, K.J., Overmann, J., Nakagawa,
786 S., Kim, J.J., Dunfield, P.F., Dedysh, S.N., Villanueva, L., 2018. An overview of the
787 occurrence of ether- and ester-linked iso-diabolic acid membrane lipids in microbial
788 cultures of the Acidobacteria: Implications for brGDGT paleoproxies for temperature and
789 pH. *Organic Geochemistry* 124, 63–76.

790 Sinninghe Damsté, J.S., Rijpstra, W.I.C., Hopmans, E.C., Foesel, B.U., Wüst, P.K., Overmann,
791 J., Tank, M., Bryant, D.A., Dunfield, P.F., Houghton, K., Stott, M.B., 2014. Ether- and
792 ester-bound iso-diabolic acid and other lipids in members of Acidobacteria Subdivision
793 4. *Applied and Environmental Microbiology* 80, 5207–5218.

794 Sollai, M., Villanueva, L., Hopmans, E.C., Reichart, G.J., Sinninghe Damsté, J.S., 2019. A
795 combined lipidomic and 16S rRNA gene amplicon sequencing approach reveals archaeal
796 sources of intact polar lipids in the stratified Black Sea water column. *Geobiology* 17, 91–
797 109.

798 Squires, M.M., Lesack, L.F.W., 2002. Water transparency and nutrients as controls on
799 phytoplankton along a flood-frequency gradient among lakes of the Mackenzie Delta,

800 western Canadian Arctic. *Canadian Journal of Fisheries and Aquatic Sciences* 59, 1339–
801 1349.

802 Squires, M.M., Lesack, L.F.W., Hecky, R.E., Guildford, S.J., Ramlal, P., Higgins, S.N., 2009.
803 Primary production and carbon dioxide metabolic balance of a lake-rich arctic river
804 floodplain: Partitioning of phytoplankton, epipelon, macrophyte, and epiphyton
805 production among lakes on the mackenzie delta. *Ecosystems* 12, 853–872.

806 Sun, Q., Chu, G., Liu, M., Xie, M., Li, S., Ling, Y., Wang, X., Shi, L., Jia, G., Lü, H., 2011.
807 Distributions and temperature dependence of branched glycerol dialkyl glycerol
808 tetraethers in recent lacustrine sediments from China and Nepal. *Journal of Geophysical*
809 *Research* 116, 1–12.

810 Tank, S.E., 2009. Sources and Cycling of Dissolved Organic carbon across a lanscape of arctic
811 delta lakes.

812 Tank, S.E., Lesack, L.F.W., Hesslein, R.H., 2008. Northern Delta lakes as summertime CO₂
813 absorbers within the arctic landscape. *Ecosystems* 12, 144–157.

814 Tank, S.E., Lesack, L.F.W., Mcqueen, D.J., 2009. Elevated pH regulates bacterial carbon
815 cycling in lakes with high photosynthetic activity. *Ecology* 90, 1910–1922.

816 Tierney, J.E., Russell, J.M., 2009. Distributions of branched GDGTs in a tropical lake system:
817 Implications for lacustrine application of the MBT/CBT paleoproxy. *Organic*
818 *Geochemistry* 40, 1032–1036.

819 Tierney, J.E., Russell, J.M., Eggermont, H., Hopmans, E.C., Verschuren, D., Sinninghe
820 Damsté, J.S., 2010. Environmental controls on branched tetraether lipid distributions in
821 tropical East African lake sediments. *Geochimica et Cosmochimica Acta* 74, 4902–4918.

822 Valentine, D.L., Chidthaisong, A., Rice, A., Reeburgh, W.S., Tyler, S.C., 2004. Carbon and
823 hydrogen isotope fractionation by moderately thermophilic methanogens. *Geochimica et*
824 *Cosmochimica Acta* 68, 1571–1590.

825 Villanueva, L., Damsté, J.S.S., Schouten, S., 2014. A re-evaluation of the archaeal membrane
826 lipid biosynthetic pathway. *Nature Reviews Microbiology* 12, 438–448.

827 Vonk, J.E., Drenzek, N.J., Huguen, K.A., Stanley, R.H.R., McIntyre, C., Montluçon, D.B.,
828 Giosan, L., Southon, J.R., Santos, G.M., Druffel, E.R.M., Andersson, A.A., Sköld, M.,
829 Eglinton, T.I., 2019. Temporal deconvolution of vascular plant-derived fatty acids
830 exported from terrestrial watersheds. *Geochimica et Cosmochimica Acta* 244, 502–521.

831 Vonk, J.E., Giosan, L., Blusztajn, J., Montluçon, D., Graf Pannatier, E., McIntyre, C., Wacker,
832 L., Macdonald, R.W., Yunker, M.B., Eglinton, T.I., 2015. Spatial variations in
833 geochemical characteristics of the modern Mackenzie Delta sedimentary system.
834 *Geochimica et Cosmochimica Acta* 171, 100–120.

835 Watson, B.I., Williams, J.W., Russell, J.M., Jackson, S.T., Shane, L., Lowell, T. V., 2018.
836 Temperature variations in the southern Great Lakes during the last deglaciation:
837 Comparison between pollen and GDGT proxies. *Quaternary Science Reviews* 182, 78–
838 92.

839 Weber, Y., De Jonge, C., Rijpstra, W.I.C., Hopmans, E.C., Stadnitskaia, A., Schubert, C.J.,
840 Lehmann, M.F., Sinninghe Damsté, J.S., Niemann, H., 2015. Identification and carbon
841 isotope composition of a novel branched GDGT isomer in lake sediments: Evidence for
842 lacustrine branched GDGT production. *Geochimica et Cosmochimica Acta* 154, 118–129.

843 Weber, Y., Sinninghe Damsté, J.S., Zopfi, J., De Jonge, C., Gilli, A., Schubert, C.J., Lepori,
844 F., Lehmann, M.F., Niemann, H., 2018. Redox-dependent niche differentiation provides
845 evidence for multiple bacterial sources of glycerol tetraether lipids in lakes. *Proceedings*
846 *of the National Academy of Sciences* 115, 10926–10931.

847 Weijers, J.W.H., Schouten, S., van den Donker, J.C., Hopmans, E.C., Damsté, J.S.S., 2007.
848 Environmental controls on bacterial tetraether membrane lipid distribution in soils.
849 *Geochimica et Cosmochimica Acta* 71, 703–713.

850 Weijers, J.W.H., Wiesenberg, G.L.B., Bol, R., Hopmans, E.C., Pancost, R.D., 2010. Carbon
851 isotopic composition of branched tetraether membrane lipids in soils suggest a rapid
852 turnover and a heterotrophic life style of their source organism(s). *Biogeosciences* 7,
853 2959–2973.

854 Whitticar, M.J., Faber, E., Schoell, M., 1986. Biogenic methane formation in marine and
855 freshwater environments: CO₂ reduction vs. acetate fermentation-Isotope evidence.
856 *Geochimica et Cosmochimica Acta* 50, 693–709.

857 Xiao, W., Wang, Y., Zhou, S., Hu, L., Yang, H., Xu, Y., 2016. Ubiquitous production of
858 branched glycerol dialkyl glycerol tetraethers (brGDGTs) in global marine environments:
859 A new source indicator for brGDGTs. *Biogeosciences* 13, 5883–5894.

860 Yang, H., Lü, X., Ding, W., Lei, Y., Dang, X., Xie, S., 2015. Organic Geochemistry The 6-
861 methyl branched tetraethers significantly affect the performance of the methylation index
862 (MBT 0) in soils from an altitudinal transect at Mount Shennongjia. *Organic*
863 *Geochemistry* 82, 42–53.

864 Zhang, Y.G., Zhang, C.L., Liu, X.L., Li, L., Hinrichs, K.U., Noakes, J.E., 2011. Methane
865 Index: A tetraether archaeal lipid biomarker indicator for detecting the instability of
866 marine gas hydrates. *Earth and Planetary Science Letters* 307, 525–534.

867 Zink, K.G., Vandergoes, M.J., Bauersachs, T., Newnham, R.M., Rees, A.B.H., Schwark, L.,
868 2016. A refined paleotemperature calibration for New Zealand limnic environments using
869 differentiation of branched glycerol dialkyl glycerol tetraether (brGDGT) sources. *Journal*
870 *of Quaternary Science* 31, 823–835.

871